stretched above T_g do not allow the question to be answered.

Acknowledgment. The financial support of the Swiss National Science Foundation is gratefully acknowledged. We thank Prof. P. J. Flory for fruitful discussions and are indebted to Dr. B. J. Schmitt (BASF AG) and Dr. W. Wunderlich (Röhm GmbH.) for providing the deuteriomethyl methacrylate. The GPC measurements of low molecular weight PMMA were kindly performed by Dr. M. Stickler (Röhm GmbH.). We are also indebted to Dr. R. E. Ghosh and Dr. A. Wright (ILL, Grenoble) for their help with the experiments and data evaluation.

Registry No. PMMA (homopolymer), 9011-14-7; neutron, 12586-31-1.

References and Notes

(1) Ward, I. M. "Mechanical Properties of Solid Polymers"; Wiley-Interscience: New York, 1983.
(2) Kausch, H. H. "Polymer Fracture", 1st ed.; Springer-Verlag: Berlin, 1978 (2nd ed. to be published).
(3) Donald, A. M.; Kramer, E. J. *Polymer* **1982**, *23*, 1183.
(4) Donald, A. M.; Kramer, E. J. *J. Polym. Sci., Polym. Phys. Ed.* **1982**, *20*, 899.
(5) Lefebvre, J. M.; Escaig, B.; Picot, C. *Polymer* **1982**, *23*, 1751.
(6) Kirste, R. G.; Kruse, W. A.; Ibel, K. *Polymer* **1975**, *16*, 120.
(7) (a) Timmins, P. A.; May, R. P. ILL Internal Report 81 TI 535. (b) Maier, B., Ed. "Neutron Research Facilities at the ILL High Flux Reactor"; Institut Laue-Langevin: Grenoble, France, Dec 1983.
(8) Ghosh, R. E. ILL Internal Report 81 GH 29T.
(9) Tangari, C.; Summerfield, G. C.; King, J. S.; Berliner, R.; Mildner, D. F. R. *Macromolecules* **1980**, *13*, 1546.
(10) Gawrisch, W.; Brereton, M. G.; Fischer, E. W. *Polym. Bull.* **1981**, *4*, 687.
(11) Benoit, H.; Duplessix, R.; Ober, R.; Daoud, M.; Cotton, J. P.; Farnoux, B.; Jannink, G. *Macromolecules* **1975**, *8*, 451.
(12) Pearson, D. S. *Macromolecules* **1977**, *10*, 696.
(13) Ullman, R. *J. Chem. Phys.* **1979**, *71*, 436.
(14) Rehage, G.; Goldbach, G. *Angew. Makromol. Chem.* **1967**, *9*, 125.
(15) Allison, S. W.; Andrews, R. D. *J. Appl. Phys.* **1967**, *38*, 4164.
(16) Beardmore, P. *Philos. Mag.* **1969**, *19*, 389.
(17) Matsushige, K.; Radcliffe, S. V.; Baer, E. *J. Appl. Polym. Sci.* **1976**, *20*, 1853.
(18) Kahar, N.; Duckett, R. A.; Ward, I. M. *Polymer* **1978**, *19*, 136.
(19) Kambour, R. P. *Polymer* **1964**, *5*, 143.
(20) Dettenmaier, M. *Adv. Polym. Sci.* **1983**, *52/53*, 57.
(21) Summerfield, G. C. *J. Polym. Sci., Polym. Phys. Ed.* **1981**, *19*, 1011.
(22) Tangari, C.; King, J. S.; Summerfield, G. C. *Macromolecules* **1982**, *15*, 132.
(23) O'Reilly, J. M.; Teegarden, D. M.; Wignall, G. D. *Macromolecules* **1985**, *18*, 2747.
(24) Picot, C.; Duplessix, R.; Decker, D.; Benoit, H.; Boué, F.; Cotton, J. P.; Daoud, M.; Farnoux, B.; Jannink, G.; Nierlich, M.; de Vries, A. J.; Pincus, P. *Macromolecules* **1977**, *10*, 436.
(25) Maconnachie, A.; Allen, G.; Richards, R. W. *Polymer* **1981**, *22*, 1157.
(26) Boué, F.; Nierlich, M.; Jannink, G.; Ball, R. *J. Phys. (Paris)* **1982**, *43*, 137.
(27) Hadziioannou, G.; Wang, L.-H.; Stein, R. S.; Porter, R. S. *Macromolecules* **1982**, *15*, 880.
(28) Yoon, D. Y.; Flory, P. J. *Macromolecules* **1976**, *9*, 299.
(29) Yoon, D. Y.; Suter, U. W.; Sundararajan, P. R.; Flory, P. J. *Macromolecules* **1975**, *8*, 784.
(30) Yoon, D. Y.; Flory, P. J. *Polymer* **1975**, *16*, 645.
(31) Yoon, D. Y.; Flory, P. J. *J. Polym. Sci., Polym. Phys. Ed.* **1976**, *14*, 1425.

Brillouin Scattering and Side-Group Motions of Poly(alkyl methacrylates) above and below the Glass Transition

B. Y. Li,[†] D. Z. Jiang,[‡] G. Fytas,[§] and C. H. Wang*

Department of Chemistry, University of Utah, Salt Lake City, Utah 84112.
Received September 24, 1985

ABSTRACT: The effect of side-group motions on the Rayleigh–Brillouin spectra of poly(alkyl methacrylates) has been investigated. Various samples of poly(methyl methacrylate), poly(ethyl methacrylate), and poly(butyl methacrylate) with different molecular weights and different T_g are used to investigate (1) the relation between the Brillouin line width maximum and T_g, (2) the effect of main-chain and side-group motions on the Brillouin linewidth, and (3) the temperature dependence of the Landau–Placzek ratio. To further demonstrate the effect of side-group motion in poly(butyl methacrylate) (PBMA), Brillouin scattering of stretched PBMA films has also been investigated.

Introduction

The use of light scattering to study amorphous solids (glasses) dates back to the time of Lord Rayleigh[1] and has continued to the present day with every increasing activity. However, it is the development of modern optical techniques involving the use of a single-mode laser for excitation and a Fabry–Perot interferometer or a digital correlator for spectral analysis that makes it feasible to obtain information about the dynamic processes underlying formation of the glass state.

Dynamic light scattering from an isotropic medium (liquid or glass) arises from thermodynamic fluctuations in the local density, anisotropy, and, in the case of a multicomponent system, concentration. These fluctuations give rise to variations in the local dielectric constant tensor. In a light scattering experiment dealing with an amorphous system, the wavelength of the laser light employed for excitation is long compared with the intermolecular distance; it is thus useful to treat the scattering system as a continuous medium in which thermally excited collective excitations perturb the local dielectric constant tensor. For an isotropic medium such as the poly(alkyl methacrylate) system presently considered in this paper, the dominant contribution to the light scattering intensity arises from density fluctuations, as the contribution from anisotropy fluctuations to the scattered light is negligible. The scattering spectrum arising from density fluctuations is known as the Rayleigh–Brillouin spectrum.

The Rayleigh–Brillouin spectrum from a polymer melt consists of a central component and a pair of shifted sidebands. The intensity ratio between the central com-

[†] Institute of Applied Chemistry, Academia Sinica, Changchun, Jilin, China.
[‡] Department of Chemistry, Jilin University, Changchun, Jilin, China.
[§] Department of Chemistry, University of Crete, Iraklion, Crete, Greece.

0024-9297/86/2219-0778$01.50/0

ponent (I_C) and the side bands ($2I_B$) is known as the Landau–Placzek ratio (LPR). However, in a polymer melt, a considerable intensity distribution centered about the central component is also present in the spectrum. This additional intensity distribution, known as the Mountain component, is associated with the relaxation behavior of the longitudinal stress modulus.[2] In the polymer melt, the longitudinal stress modulus is relaxed mainly through the pathway of structural relaxation involving movements of small segments in the polymer chain, although in some cases the coupling of low-lying intramolecular vibrational modes giving rise to specific heat relaxation may also contribute.[3] Because of the presence of the Mountain component, the usual definition of the LPR has to be modified. The modification will be discussed in the later section.

To understand the dispersion behavior present in the Rayleigh–Brillouin spectrum, the "secondary" main-chain relaxation has been proposed.[4] This assignment is consistent with the picture that the Rayleigh–Brillouin spectrum of a polymer melt is associated with localized segmental motions. However, as has been pointed out in our recent article,[5] the loss or dispersive mechanism present in the Brillouin spectrum is not restricted to the main-chain relaxation. Other types of secondary relaxation processes such as side-group motions may in some cases play a dominant role in affecting the Rayleigh–Brillouin spectrum.

The purpose of this paper is to demonstrate the importance of the side-group motions in a polymer chain in the Rayleigh–Brillouin spectrum. We use different poly(alkyl methacrylates) polymers having several molecular weights and glass temperatures (T_g) as examples. Eight samples are used in the studies: three poly(methyl methacrylate) or PMMA (M_w = 3900, T_g = 7 °C; M_w = 60 000, T_g = 85 °C; $M_w \simeq 10^7$, T_g = 107 °C), two poly(ethyl methacrylate) or PEMA (M_w = 2500, T_g = 10 °C; M_w = 16 000, T_g = 34 °C), and three poly(*n*-butyl methacrylate) or PBMA (M_w = 3500, T_g not well defined; M_w = 31 000, T_g = 8 °C; M_w = 75 000, T_g = 17 °C). These samples are chosen because they form amorphous glass systems, and the results of the Brillouin studies of these systems will allow us to comment on (1) the relation of T_g with the temperature at which the Brillouin line width is maximum; (2) the effect of main-chain and side-group motions on the Brillouin line width; (3) the temperature dependence of the Landau–Placzek ratio. Such information is very useful in understanding the dynamic behavior of the glass transition in the amorphous polymer system.

To further demonstrate the dominance of the side-group motion in PBMA, we have also carried out Brillouin scattering measurements of PBMA films stretched to various stretch ratios. In contrast to other amorphous polymer systems such as polycarbonate films that have been studied in this laboratory, stretching does not result in orientation of the PBMA films as the chain orientation induced by stretching relaxes very quickly by the side-group motion. As a result, the hypersonic velocities of the PBMA films stretched to various stretch ratios remain practically unchanged.

Experimental Section

The Rayleigh–Brillouin spectra were obtained in the VV scattering configuration with an etalon-selected single-mode argon ion laser radiating at approximately 4880 Å as the excitation radiation source. The laser power at the sample was about 300 mW. The scattered light from the sample was spectrally analyzed with a piezoelectrically scanned five-pass Fabry–Perot interferometer. A Burleigh DAS-1 stabilization system was used to maintain the finesse of the Fabry–Perot interferometer by stablizing the Fabry–Perot cavity length and also compensating the laser frequency shift. In some instances, the free spectral range, adjusted to about three times the Brillouin shift, was used to record the spectrum of each sample at a particular temperature. For example, for PMMA below 20 °C, the free spectral range was 40.65 GHz, and above 20 °C the free spectral range was set at 26.18 GHz. The finesse of the optical system was higher than 90 for all spectral runs.

Table I
Brillouin Scattering Results of PMMA-3 (M_w = 10^7) at Various Temperatures (Data Were Obtained by Heating)

T/°C	V_l/(m s^{-1})	$2\Gamma_B$/MHz	LPR
−26	2972 ± 19	111 ± 28	13.3
1	2916	171 ± 28	12.9
20	2857	161 ± 28	12.2
42	2806	137 ± 22	13.3
61	2745	158 ± 20	11.5
85	2652	180 ± 15	11.6
104	2576	230 ± 12	9.0
134	2380	307 ± 10	7.2
153	2207	439 ± 16	6.9
177	2017	569 ± 10	5.0
199	1892	679 ± 25	3.8
214	1758	891 ± 18	3.3
234	1621	1093 ± 19	3.0
253	1455	1279 ± 24	2.6
262	1394	1400 ± 38	2.6

All samples were kindly provided by Dr. W. Wunderlich, Rohm GmbH Darmstadt, West Germany. The molecular weight data of all samples were provided by Rohm GmbH Darmstadt through the standard techniques of light scattering and GPC. The glass temperature of each sample was determined with a DSC apparatus available at the Universitat Bielefeld, West Germany. Except for PMMA-3, the highest molecular weight PMMA sample, all samples were cleaned and purified by first dissolving the polymer in benzene. The solution was then filtered through a 0.22-μm Millipore filter to remove dust, and a controlled freeze–dry method was used to remove the solvent. The sample was then annealed in a vacuum oven above T_g to obtain an optically clear, homogeneous, and strain-free specimen. To ascertain that the solvent was indeed completely removed, a DSC scan was made to measure the glass temperature of the purified sampled. The PMMA-3 sample was cut and polished from a commercial plate provided by Rohm GmbH Darmstadt, West Germany, without further purification. The commercial PMMA-3 appears optically homogeneous, with only a slightly higher LPR when the result is compared with that of PMMA-2. (See Table I.)

PBMA films were prepared by a melt-casting technique similar to that described in ref 6. The purified PBMA sample (T_g = 27 °C) was heated between two plates in a hydraulic press at a temperature of 162 °C and a pressure of 1 metric ton for above 5 min. The films obtained were then quenched in ice water. The optically clear films were stretched at room temperature (23.5 °C), but in order to prepare films with stretch ratios (R_s) greater than 4, they were heated to 34 °C during stretching.

The Brillouin spectra of the films at different stretch ratios were obtained by using a special 90° scattering geometry[9] with the film bisecting the angle subtended by the incident and the scattered beams. Temperature-dependent studies of PBMA films were carried out with R_s = 1 and R_s = 2.5 films.

Theoretical Background

The Rayleigh–Brillouin spectrum observed at the scattering angle θ is proportional to the fourier transform of the qth mode of the density–density correlation function given by

$$C(\mathbf{q},t) = \langle|\delta\rho(\mathbf{q},t)\delta\rho^*(\mathbf{q})|\rangle \quad (1)$$

where the amplitude of the scattering vector $\mathbf{q}$ is equal to $q = |\mathbf{q}| = (4\pi n/\lambda)\sin(\theta/2)$, n being the index of refraction of the medium at the incident wavelength in vacuum. The density fluctuation $\delta\rho(\mathbf{q},t)$ is given by

$$\delta\rho(\mathbf{q},t) = \sum_j e^{i\mathbf{q}\cdot\mathbf{r}_j(t)} \quad (2)$$

where r_j is the position of the polymer segment j responsible for light scattering. For amorphous polymers, the density fluctuation depends only on the amplitude and not the direction of the scattering vector.

If the normalized Rayleigh–Brillouin spectral density is given as

$$\hat{I}(\mathbf{q},\omega) = \frac{1}{2\pi}\int_{-\infty}^{\infty} dt\, e^{-i\omega t} C(\mathbf{q},t)/C(\mathbf{q},0) \tag{3}$$

it can be shown that $\hat{I}(\mathbf{q},\omega)$ is related to the dynamic compliance spectrum by[7]

$$\hat{I}(\mathbf{q},\omega) = \left(\frac{1}{\chi_\infty}\right)\frac{D''(\mathbf{q},\omega)}{\omega} \tag{4}$$

where χ_∞ is the high-frequency isothermal compressibility and $D''(\mathbf{q},\omega)$ is the imaginary part of the dynamic longitudinal compliance. The q dependence in $D''(q,\omega)$ is unimportant for $\omega \leq 10$ MHz. However, at higher frequency, the acoustic phonon contributes to the scattering spectrum and the q dependence is related to ω by the sound dispersion relation.

The thermodynamic sum rule[8] gives the total integrated intensity proportional to

$$\frac{1}{\pi}\int_{-\infty}^{\infty} d\omega \frac{D''(q,\omega)}{\omega} = \frac{\beta}{V\rho_0^2}\langle|\delta\rho(\mathbf{q})|^2\rangle \tag{5}$$

where $\beta = 1/kT$, ρ_0 is the equilibrium number density, and V is the scattering volume.

It can be shown[2] that the high-frequency unrelaxed isothermal sound velocity $V_T(\mathbf{q})$ is equal to $(NkT/m)^{1/2}\cdot\langle|\delta\rho(\mathbf{q})|^2\rangle^{-1/2}$, where m and N are, respectively, the mass and the number of the scattering unit. In the limit of vanishing q (or low frequency), the isothermal sound velocity V_T reduces to $(\rho_m\chi_T)^{-1/2}$, where ρ_m is the mass density and χ_T is the isothermal compressibility. Brillouin scattering yields the adiabatic sound veloicity due to the coupling of the acoustic phonon to the energy fluctuation.

To obtain the hypersonic longitudinal velocity $V_l(q)$ from Brillouin scattering, one measures the frequency shift f_B (in Hz) and deduces $V_l(q)$ from the expression

$$V_l(\mathbf{q}) = f_B/q \tag{6}$$

which reduces to

$$V_l(\mathbf{q}) = f_B\lambda/2^{1/2} \tag{7}$$

in the special 90° scattering geometry used when the film is oriented at 45° with respect to the incident beam.[9] Note that in this special geometry, the refractive index n does not appear in eq 7.

At low temperature when the structural relaxation time is so long $V_l(\mathbf{q})$ has a simple relationship to $V_T(\mathbf{q})$. At high temperature when the relaxation time is short, $V_l(\mathbf{q})$ also has a simple relationship to $V_T(\mathbf{q})$. In between $V_l(\mathbf{q})$ is affected by the structural relaxation process. Investigation of the structural relaxation process is best carried out by the light-beating photon correlation technique. Application of this technique to PMMA,[10] PEMA,[11,12] and PBMA[13] has been reported in the literature. In a separate publication, we shall also present new results of photon correlation studies of the structural relaxation component in PMMA.[14]

Results and Discussion

Comparison of the Brillouin spectra of PMMA, PEMA, and PBMA at 20 °C are given in Figure 1. PMMA-2 has a T_g = 85 °C, thus the spectrum displayed for PMMA-2 is below T_g. The PBMA-3 spectrum is near T_g (=17 °C) and the PEMA-1 spectrum is above T_g (=−10 °C). One notes that although the PBMA-3 spectrum is only taken at 3 °C above T_g, a large Brillouin spectral line width is already apparent.

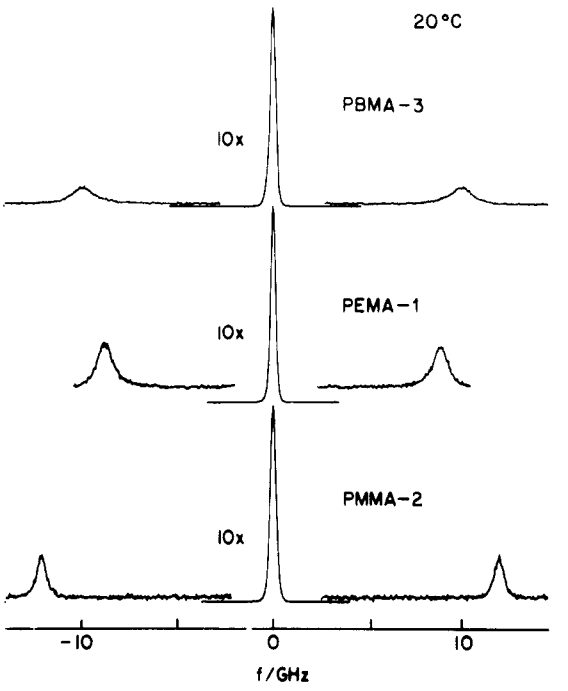

Figure 1. Brillouin spectra of PMMA (T_g = 85 °C), PEMA (T_g = −10 °C), and PBMA (T_g = 17 °C) at 20 °C.

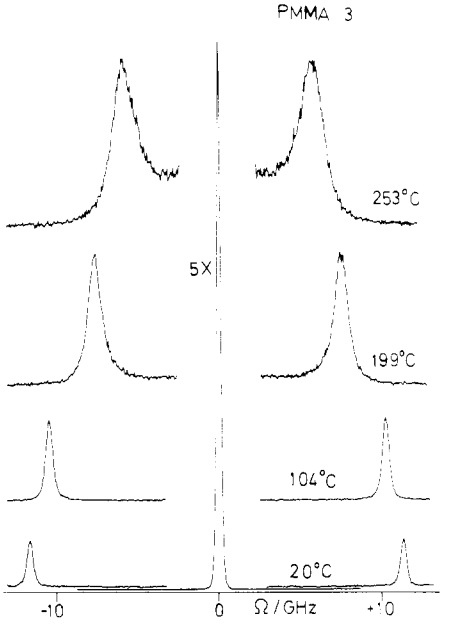

Figure 2. Brillouin spectra of PMMA-3 (T_g = 110 °C) at various temperatures.

The Brillouin spectra of PMMA-3 at various temperatures are shown in Figure 2. When the sample temperature is increased, the line width increases gradually, accompanied by shifting of the peak frequency to a lower value. Over the temperature range between 20 and 90 °C, the central Rayleigh component is instrumentally limited. However, above T_g (=110 °C), the Mountain component appears and becomes rather pronounced at higher temperature, as clearly shown by 253 °C spectrum, in which a large scattering intensity distribution is found between the two Brillouin peaks.

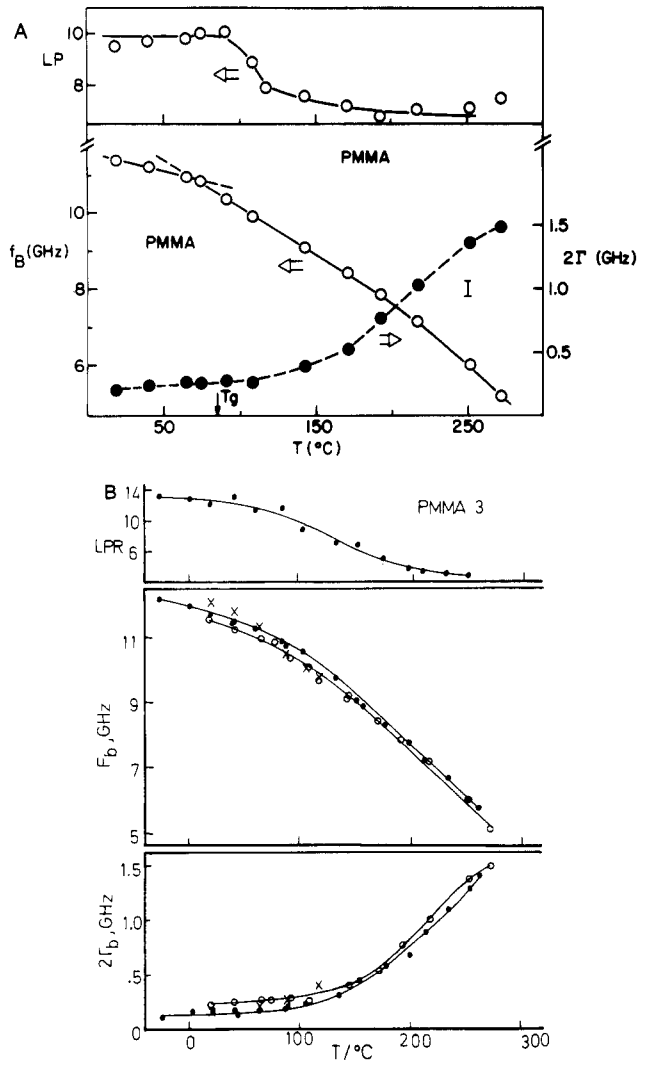

Figure 3. (A) Temperature dependence of the Brillouin data (frequency shift, line width, and the Landau–Placzek ratio (labeled as LP of PMMA-2; T_g = 85 °C). (B) Temperature dependence of the Brillouin data (frequency shift and line width) for all three PMMA samples. The LPR data presented in this figure is for PMMA-3. Data for PMMA-1 is indicated by crosses, PMMA-2 by open circles, and PMMA-3 by solid circles.

The temperature dependence of the Brillouin shift (f_B), line width (2Γ, the whole width at half-height), and the LPR of PMMA-2 are shown in Figure 3A. As the temperature is increased, the Brillouin shift decreases nonlinearly, accompanied by the line width increase, and without displaying any anomalous change at T_g. The Landau–Placzek ratio decreases slightly with increasing temperature above 150 °C; below this temperature, it increases rapidly with decreasing temperature, reaching an apparent plateau value about 10 °C below T_g. Because of the presence of the Mountain component, to obtain the LPR, the Brillouin intensity I_B is taken as twice the intensity integrated from the Brillouin peak to the high-frequency portion and the central peak intensity I_C is the difference between the total integrated intensity and $2I_B$. By this modification, the contribution of the Mountain component is included in the calculation of the LPR.

The temperature dependence of the Brillouin data of three PMMA samples is summarized in Figure 3B, the LPR of PMMA-3 displayed at the top of the figure. One notes that, except for a slightly higher LPR value for PMMA-3 below T_g as compared with that for PMMA-2, shown in Figure 3A, and in spite of different molecular weights, the temperature dependence of the frequency shift, line width, and LPR data for three PMMA samples is quite similar.

The Brillouin scattering spectrum of amorphous PMMA studied as a function of temperature has been reported by several workers.[15-24] Only the velocity data are reported in ref 15 and 16; ref 17 and 18 present both the frequency (velocity) and the hypersonic attenuation data. References 19 and 20 deal with low temperature in the range 4–300 K (~27 °C). Over the 20–150 °C range our velocity data agree with that of ref 17 to about 3%. No Brillouin data higher than 140 °C have hitherto been reported. At room temperature our value for V_l is 2857 ± 19 m/s, and for the attenuation coefficient α ($=2\pi\Gamma_B/V_l$, Γ_B is the half-width at half-height in Hz) 1.7×10^3 cm^{-1} at 11.7 GHz, in contrast to V_l = 2760 m/s and $\alpha = 2.8 \times 10^3$ cm^{-1} at about the same frequency reported in ref 17. At 20 °C our value for the attenuation coefficient over one wavelength ($\alpha\Lambda_s$) is 2.14 $\times 10^{-2}$ cm^{-1}, in contrast to 7.0×10^{-2} cm^{-1} reported in ref 17. The half-line-width (Γ_B) data reported in ref 18 over the range 40–140 °C are about a factor of 2 larger than the present result. If Γ_B reported in ref 18 was interpreted as the whole width, rather than the half-width as there stated, it would be an agreement. The LPR reported in ref 17 is 20 at room temperature, in contrast to the present 12.2 for PMMA-3 and 8.9 for the PMMA-2 sample that we have observed. The gradual increase of the LPR to an asymptotic plateau value as the temperature is decreased below T_g for PMMA has not been shown. Comparison of the present PMMA data with those previously given indicates that our results are more accurate. The greater accuracy is indicated by a lower LPR, achieved by a careful sample preparation procedure employed to remove static inhomogeneity. The high-quality spectra are obtained by a very high finesse interferometer through active control using an electronic stabilization system.

We now turn to PEMA. The temperature dependence of the Brillouin data of two PEMA samples is shown in Figure 4. PEMA-2 displays a characteristic kick in the Brillouin frequency at T_g ($T_{g,2}$ = 34 °C). Our notes that over the temperature range 0–200 °C, a lower frequency and a greater line width are found for the low molecular weight sample (PEMA-1). The lower frequency and larger line width results suggest a greater free volume fluctuation present in the low molecular weight PEMA sample.

In contrast to the result of PMMA, the line width Γ_B of both samples display a broad maximum, with the position of the maximum for the low molecular weight sample occurring at lower temperature. Comparison with the PEMA result shows that the line width maximum of PMMA probably also occurs but at a temperature higher than the sample degradation temperature. The Landau–Placzek ratio, which is lower for the low molecular weight sample, also displays a characteristic rise on lowering the temperature toward T_g, similar to that found in PMMA.

The temperature dependence of the hypersonic velocity of PEMA in the temperature range 20–100 °C has been reported in ref 15. The frequency shift and the half-width data of PEMA at low temperature from 10 to 300 K have also recently been reported.[20] Below T_g, our Brillouin line width is found to be insensitive to the temperature variation, in agreement with the result of ref 20.

Results of the Brillouin spectral studies of three PBMA samples are shown in Figure 5. The hypersonic frequencies of PBMA-2 and PBMA-3 are basically the same, despite differences in T_g. The Brillouin line widths of those two samples above T_g are also quite similar; however, below T_g PBMA-3 has a greater line width than PBMA-2. The lowest molecular weight sample (PBMA-1) behaves

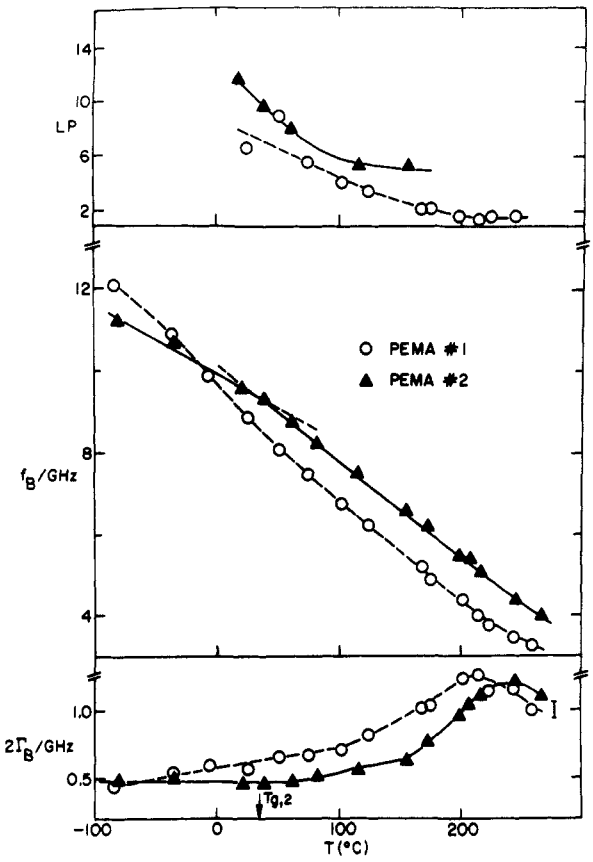

Figure 4. Temperature dependence of the Brillouin data (frequency shift, line width, and LPR) of two PEMA samples (labeled as PEMA 1 and 2 for PEMA-1 and PEMA-2, respectively).

differently from the other two. The results of lower Brillouin frequency and larger line width found in the lowest molecular weight PBMA again indicate a greater free volume fluctuation of this low molecular weight sample. For PBMA-1, one may imagine a broad line width maximum around 65 °C. There is apparently no maximum in the other higher T_g samples. Below 0 °C PBMA-1 (M_w = 3500, M_n = 1900) and PBMA-2 (M_w = 31 100, M_n = 11 100) have practically the same temperature dependence in both f_B and Γ_B. One notes that above −50 °C, the Brillouin frequency of the low molecular weight sample (PBMA-1) is lower than the other two, but it becomes higher than the others below −50 °C. The LPR data increase with decreasing temperature, but no systematic trend is found for the PBMA samples.

The temperature dependence of the hypersonic velocity and attenuation coefficient over the temperature range 23–142 °C for two PBMA films (T_g = 17 °C, stretched R_s = 2.5 and unstretched R_s = 1.0) are shown in Figure 6. The sound velocity was obtained by using eq 7. The attenuation coefficient per hypersonic wavelength, $\alpha\Lambda_s$, is calculated from the line width and hypersonic data by using the equation

$$\alpha\Lambda_s = \pi\Gamma_B/f_B \tag{8}$$

The shape of the hypersonic velocity curves for the stretched and unstretched films are quite similar to that given for the PBMA-3 sample shown in Figure 5; there appears to be no difference in these two films. The attenuation coefficients $\alpha\Lambda_s$ obtained for the two films do not show a maximum, and, within the experimental uncertainty, there appears to be no difference in the $\alpha\Lambda_s$ for these two films. Moreover, the amplitude of the line width increase upon increasing temperature appears to be quite

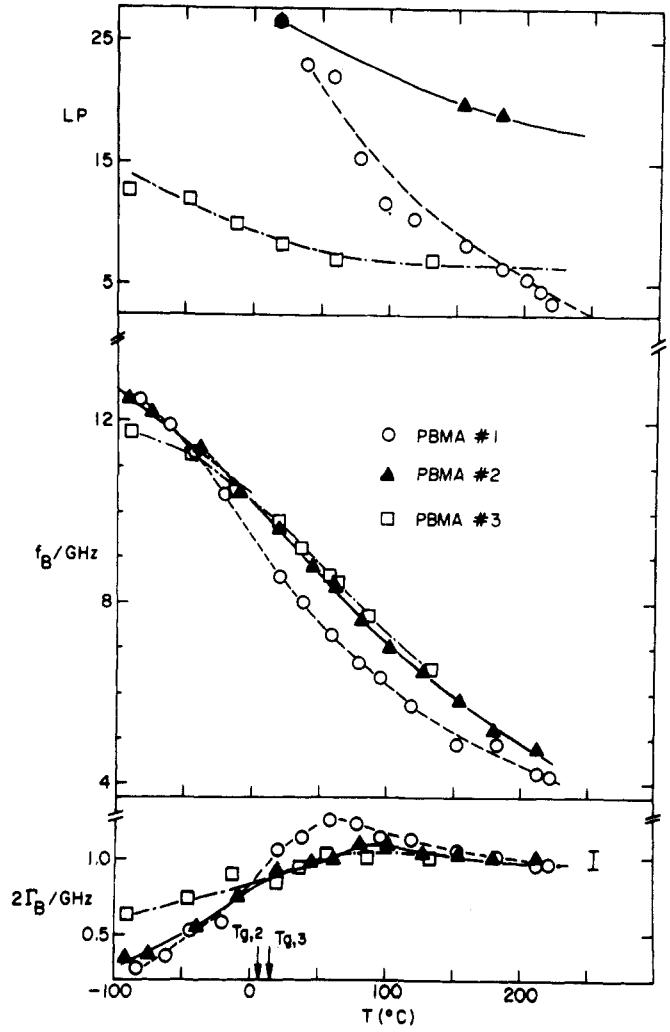

Figure 5. Temperature dependence of the Brillouin data (frequency shift and line width) of three PBMA samples.

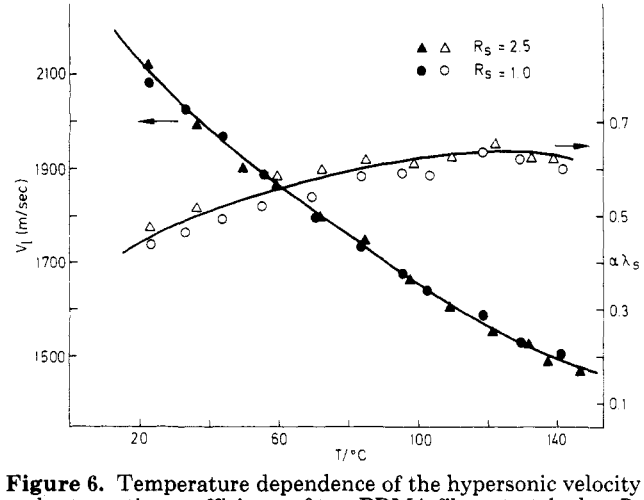

Figure 6. Temperature dependence of the hypersonic velocity and attenuation coefficients of two PBMA films stretched at R_s = 2.5 and R_s = 1. Open symbols indicate heating and solid symbols cooling the samples.

small, and the result is similar to the line width data of the rod sample, shown in Figure 5.

To summarize the above results, it is clear that over the wide temperature range studied, the sound velocity of all methacrylate polymers shows dispersion above T_g. The Brillouin line width increases gradually with increasing temperature. For PMMA, the line width maximum is not reached even at 250 °C; thus, higher temperature is needed

to observe the line width maximum. However, heating above 250 °C causes considerable degradation of the polymer. A broad line width maximum is observed for PEMA (T_g = 34 °C) at 220 °C; the maximum shifts to lower temperature for lower molecular weight PEMA. A very broad line width maximum is observed at PBMA-1 at about 65 °C; however, no clear maximum is observed in other higher molecular weight PBMA samples. In other words, the change of the Brillouin line width of poly(alkyl methacrylates) with temperature becomes less pronounced as the side group is progressively increased from PMMA through PBMA. Above T_g, the hypersonic velocity (or the Brillouin frequency) is lower for the low molecular weight sample but it becomes higher below T_g. This result is very clearly shown in PEMA and PBMA but is less obvious in PMMA.

The cause for dispersion and sound attenuation below T_g is due to several possible mechanisms. Processes such as phonon–phonon interactions and scattering of phonons from static inhomogeneties and from the strain field as well as thermally induced localized segmental motions all contribute. It is still difficult to ascertain at present which contributes the most to the line width below T_g. Additional studies are thus needed to clarify these processes. Moreover, above T_g, mechanisms that lead to mechanical loss may also contribute to the dispersion and the line width of the Brillouin line. The α process, whose characteristic relaxation frequency rises rapidly with increasing temperature due to the main-chain motion can, in principle, also make a contribution to the Brillouin line width. The highest actual mechanical measurement using the ultrasonic technique reported for PMMA gives a peak at 170 °C at 2.25 MHz.[21] Extrapolation of this result to the Brillouin frequency of 10 GHz suggests that if the α mode is responsible for the dispersive effect observed in Brillouin scattering, then the line width should peak at about 190 °C. However, our measurements have covered up to 260 °C for PMMA and the Brillouin line width still shows an increase at this temperature without any sign of reaching a maximum. This result suggests that the relaxation processes responsible for the hypersonic dispersion in PMMA is probably not due to the main-chain motion.

For the main-chain relaxation process, the dynamical data that fall on the primary glass–rubber relaxation line are known to follow the WLF equation

$$\log \tau = \log \tau_0 + B/(T - T_0) \qquad (9)$$

where τ is the mean structural relaxation time of the main-chain relaxation, T_0 is the fictitious temperature at which τ becomes infinite, and B is a parameter. Assuming that the line width maximum f_B* occurs at the temperature where the primary and secondary main-chain relaxation lines merge, Jarry and Patterson[22] have used eq 9 and predicted that the temperature of the line width maximum should occur approximately at $T_{max} = T_g + 180$ K. If this prediction is correct, then T_{max} for PMMA-2 and PMMA-3 should occur at about 250 and 280 °C, respectively and for PEMA-1 and PEMA-2, T_{max} should be at 170 and 214 °C, respectively; likewise, T_{max} for PBMA should occur at 188 °C for sample 2 and 197 °C for sample 3.

Such a prediction of T_{max} is not verified in the present poly(alkyl methacrylate) samples studied here. Neither is the prediction applicable in poly(siloxanes),[5] in which side-group motion also plays an important role.

Clearly, these results suggest that when side-group motions are present, the primary and secondary transition lines will not merge at high temperature (or high frequency). The secondary relaxation process associated with localized motion may either be due to side-group motion

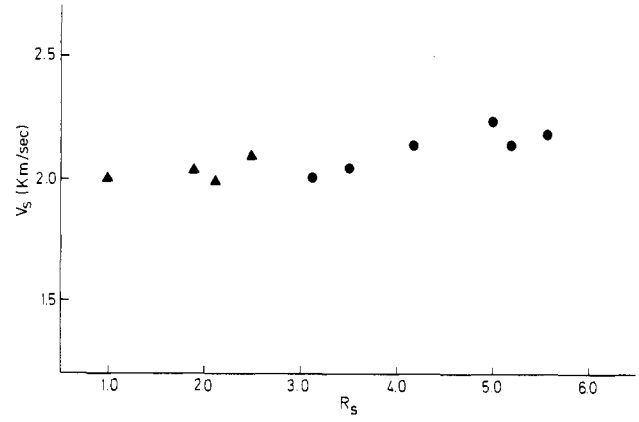

Figure 7. Hypersonic velocity of PBMA films at room temperature stretched below (solid triangles) and above (solid circles) T_g.

or to the segmental motion involving the main chain; these two appear to show different dynamic behavior in the hypersonic frequency range. Thus, in order to obtain a meaningful relation between T_{max} and T_g, specific considerations of the dynamics underlying these processes appear to be necessary. However, this is a very difficult task.

Increasing the side group of the alkyl methacrylate polymer has the effect of increasing the Brillouin line width with increasing temperature, quickly reaching the plateau value without displaying a clear line width maximum. Thus, for the type of polymers consider here, side-group motion clearly remains active over a very wide temperature range and the dynamics shows a very wide distribution of relaxation times.

The increasing importance of the side-group motion as the length of the side group is increased is best illustrated by studying the stretched films of PBMA. Figure 7 shows the hypersonic velocity of PBMA films stretched to various stretch ratios at temperatures above and below T_g. Although the data points are scattered and the sound velocity appears to increase slightly for the film with $R_s > 4.0$, no significant difference is observed for films below $R_s = 4.0$, in contrast to the results reported for PMMA in which stretching appears to decrease the hypersonic velocity.[23] However, the velocity decrease disappears when the PMMA sample is annealed.[24] The decrease in the sound velocity in PMMA is due to craze formation. The fact that stretching does not significantly change the hypersonic velocity of the PBMA film, in contrast to that observed, for example, in polycarbonate,[6] is clearly associated with the motion involving a fairly large side group.

Studies of the temperature dependence of the Landau–Placzek ratio also yield useful information about the glass transition process. According to Pinnow et al.,[25] the mean square amplitude of density fluctuations may be divided into three parts

$$\langle|\delta\rho(\mathbf{q})|^2\rangle = kT\rho_0{}^2V(\delta\chi + \chi_{s,rel} + \chi_{s,\infty}) \qquad (10)$$

where $\delta\chi$ is the difference between the low-frequency isothermal and the high-frequency adiabatic compressibility, $\chi_{s,rel}$ is the relaxational compressibility associated with structural variations, and $\chi_{s,\infty}$ is the high-frequency compressibility. In a viscoelastic material that can support high-frequency shear stress, we have $\chi_{s,\infty} = (\rho V_l{}^2)^{-1}$, where V_l is the hypersonic sound velocity.

For $\omega_s\tau \gg 1$, τ being the mean structural relaxation time, the oscillatory sound made is not coupled to the structural relaxation process; the dynamical process associated with the $\delta\chi$ and $\chi_{s,rel}$ terms will thus appear in the central

component. Neglecting the thermal diffusivity contribution, we may regard the sum of $\delta\chi$ and $\chi_{s,rel}$ simply as $\chi_{T,rel}$, the relaxing part of the isothermal compressibility. Thus, the nonpropagating density fluctuations in a viscoelastic liquid are simply proportional to $kT\chi_{T,rel}$. The time scale for these density fluctuations is determined by the structural relaxation time of the polymer melt. As the temperature is lowered, the structural relaxation becomes very long, and a glass is formed from the melt. If the rate of cooling is such that the equilibrium structure of the melt can no longer change, the density fluctuations are frozen into the newly formed solid, characterized by a fictitiuos temperature, T_f.[26] At T_f the structural relaxation time of the melt is so long that, upon lowering the temperature, no further structural rearrangement is possible. However, since the Brillouin intensity arises from the acoustic contribution, the structural contribution being negligible due to its long relaxation time, the acoustic phonon contribution will still be governed by the thermodynamic temperature T.

In view of the above discussion, Schroeder et al.[27] have argued that the mean square of the density fluctuation can be written as

$$\langle|\delta\rho(\mathbf{q})|^2\rangle = k\rho_0^2V[T_f\{\chi_{T,0} - (\rho V_l^2)^{-1}\} + T(\rho V_l^2)^{-1}] \quad (11)$$

Equation 11 shows that the intensity lost by the Brillouin peak as T_g is approached is gained by the central component through the increase intensity of the Mountain peak.

On the basis of eq 10, it follows that the Landau–Placzek ratio for the glass-forming liquid should take the form[28]

$$\text{LPR} = (T_f/T)[(\rho V_l^2)\chi_{T,0} - 1] \quad (12)$$

rather than $\gamma - 1$, as in the case of structureless liquids.[28]

Thus, by measuring the LPR, it is possible to calculate the isothermal compressibility and study its temperature dependence. Using a least-squares program to fit the LPR data of PMMA-2 to eq 12 and keeping T_f fixed, we obtain T_f = 267 K and find $\chi_{T,0}$ increases from 1.8×10^{-10} cm^2/dyn at 108 °C to 2.7×10^{-10} cm^2/dyn at 183 °C for PMMA. Below T_g, $\chi_{T,0}$ appears to be insensitive to the temperature change, and it has a value of 1.4×10^{-10} cm^2/dyn. This result is consistent with that of SiO_2 obtained by Bucaro and Dardy[29] and points to negligibly small structural changes of PMMA below T_g.

Acknowledgment. Financial support from the ONR contract and the NSF polymer program (DMR-82-16221) is appreciated. G.F. also thanks the Chemistry Department at the University of Utah for its hospitality.

Registry No. PMMA (homopolymer), 9011-14-7; PEMA (homopolymer), 9003-42-3; PBMA (homopolymer), 9003-63-8.

References and Notes

(1) Strutt, J. W. (Lord Rayleigh) *Proc. R. Soc. London A* **1919**, *A95*, 476.
(2) Huang, Y. Y.; Wang, C. H. *J. Chem. Phys.* **1974**, *62*, 120. Lin, Y. H.; Wang, C. H. *J. Chem. Phys.* **1978**, *69*, 1546.
(3) Mountain, R. D. *J. Res. Natl. Bur. Stand. Sect. A* **1966**, *70A*, 907.
(4) Patterson, G. D. *J. Polym. Sci., Polym. Phys. Ed.* **1977**, *15*, 455; **1977**, *15*, 579.
(5) Wang, C. H.; Fytas, G.; Zhang, J. *J. Chem. Phys.* **1985**, *82*, 3405.
(6) Liu, Q. L.; Wang, C. H. *Macromolecules* **1983**, *16*, 482.
(7) Wang, C. H.; Fischer, E. W. *J. Chem. Phys.* **1985**, *82*, 632.
(8) Forster, D. "Hydrodynamic Fluctuations, Broken Symmetry and Correlation Functions"; Benjamin: Reading, MA, 1975.
(9) Wang, C. H.; Cavanaugh, D. B.; Higashigaki, Y. *J. Polym. Sci., Polym. Phys. Ed.* **1981**, *19*, 941.
(10) Patterson, G. D.; Carroll, P. J.; Stevens, J. R. *J. Polym. Sci.* **1983**, *21*, 613.
(11) Patterson, G. D.; Stevens, J. R.; Lindsey, J. R. *J. Macromol. Sci., Phys.* **1980**, *B18*, 641.
(12) Fytas, G. In "Physical Optics of Dynamic Phenomena and Processes in Macromolecular Systems"; Sedlacek, B., Ed.; de Gruyter: Berlin, New York, 1985.
(13) Meier, G.; Fytas, G.; Dorfmuller, Th. *Macromolecules* **1984**, *17*, 957.
(14) Fytas, G.; Wang, C. H.; Fischer, E. W.; Mehler, K. *J. Polym. Sci., Polym. Phys. Ed.*, in press.
(15) Ronberger, A. B.; Eastman, D. P.; Hunt, J. L. *J. Chem. Phys.* **1969**, *51*, 3723.
(16) Friedman, E. A.; Ritger, A. J.; Andrew, R. D. *J. Appl. Phys.* **1969**, *40*, 4243.
(17) Jackson, D. A.; Pentecost, H. T. A.; Powles, J. G. *Mol. Phys.* **1972**, *23*, 245.
(18) Patterson, G. D. *J. Polym. Sci., Polym. Lett. Ed.* **1975**, *13*, 415.
(19) Vacher, R.; Pelous, J. *Phys. Lett.* **1976**, *58A*, 139.
(20) Kato, E.; Saji, Y. In "Physical Optics of Dynamic Phenomena and Processes in Macromolecular Systems"; Sedlacek, B., Ed.; de Gruyter: Berlin, New York, 1985.
(21) Kono, R. *J. Phys. Soc. Jpn.* **1960**, *15*, 718.
(22) Jarry, J. P.; Patterson, G. D. *J. Polym. Sci., Polym. Phys. Ed.* **1981**, *19*, 179.
(23) Yap, B.-C.; Schichijyo, S.; Matsushigi, K.; Takemura, T. *Jpn. J. Appl. Phys.* **1982**, *21*, 2523.
(24) Lindsay, S. M.; Shepherd, J. W. *J. Polym. Sci., Polym Symp.* **1977**, *No. 58*, 85.
(25) Pinnow, D. A.; Candau, J. S.; LaMachia, J. T.; Litovitz, T. A. *J. Acoust. Soc. Am.* **1968**, *43*, 131.
(26) Tobl, A. Q. *J. Am. Ceram. Soc.* **1946**, *29*, 240. Ritland, H. N. *J. Am. Ceram Soc.* **1959**, *37*, 370.
(27) Schroeder, J.; Mohr, R. K.; Macedo, P. B.; Montrose, C. J. *J. Am. Ceram Soc.* **1973**, *56*, 510.
(28) Montrose, C. J.; Silayever, V. A.; Litovitz, T. A. *J. Acoust. Soc. Am.* **1968**, *43*, 117.
(29) Bucaro, J. A.; Dardy, H. D. *J. Appl. Phys.* **1974**, *45*, 5324.